Supplement of

Assimilation of Carbonyl Sulfide (COS) fluxes within the adjoint-based data assimilation system—Nanjing University Carbon Assimilation System (NUCAS v1.0)

Huajie Zhu et al.

Correspondence to: Mousong Wu (mousongwu@nju.edu.cn)

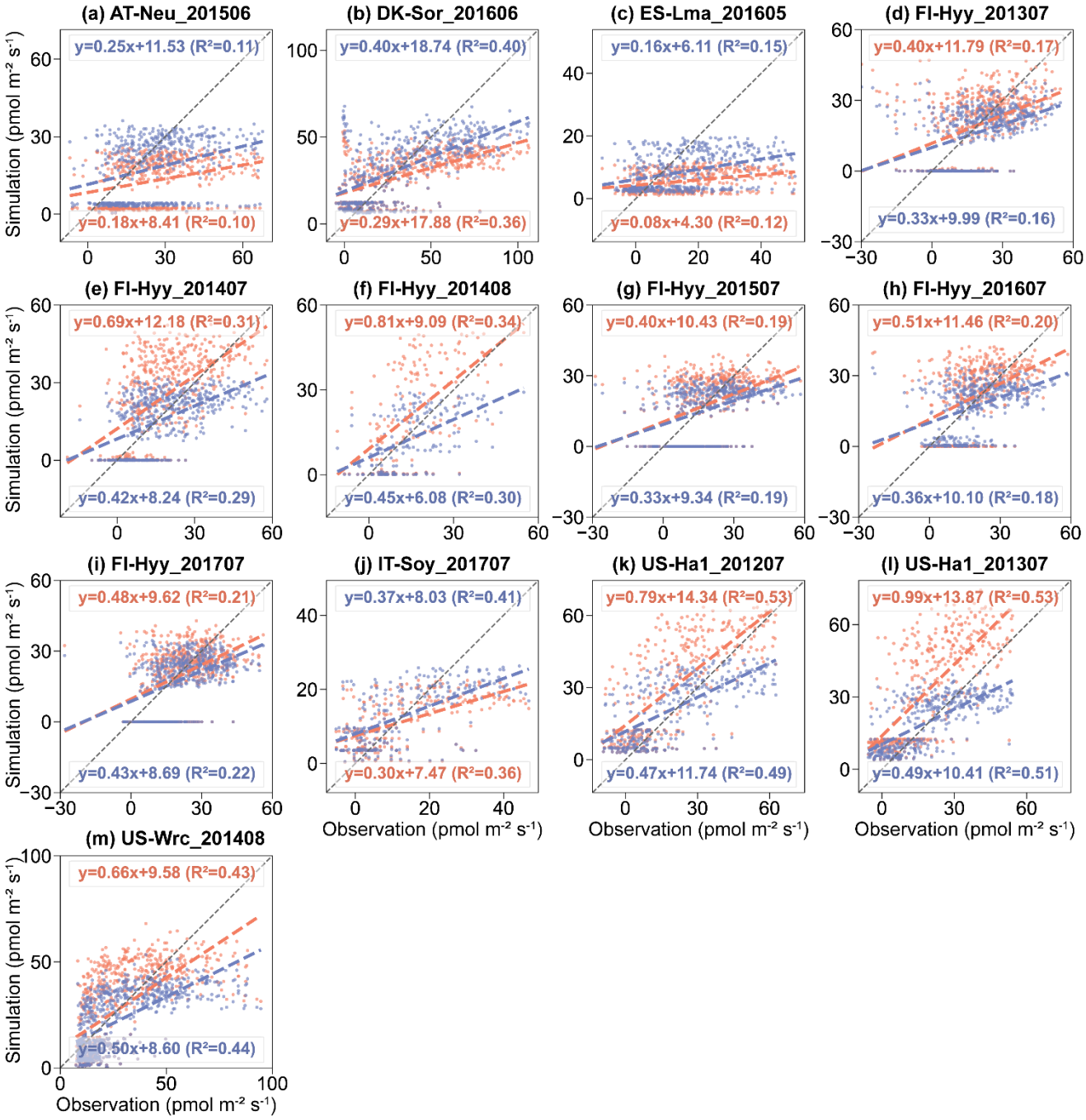

Figure S1. Scatterplots of observed versus simulated hourly COS flux using prior (red) and single-site posterior (blue) parameters.

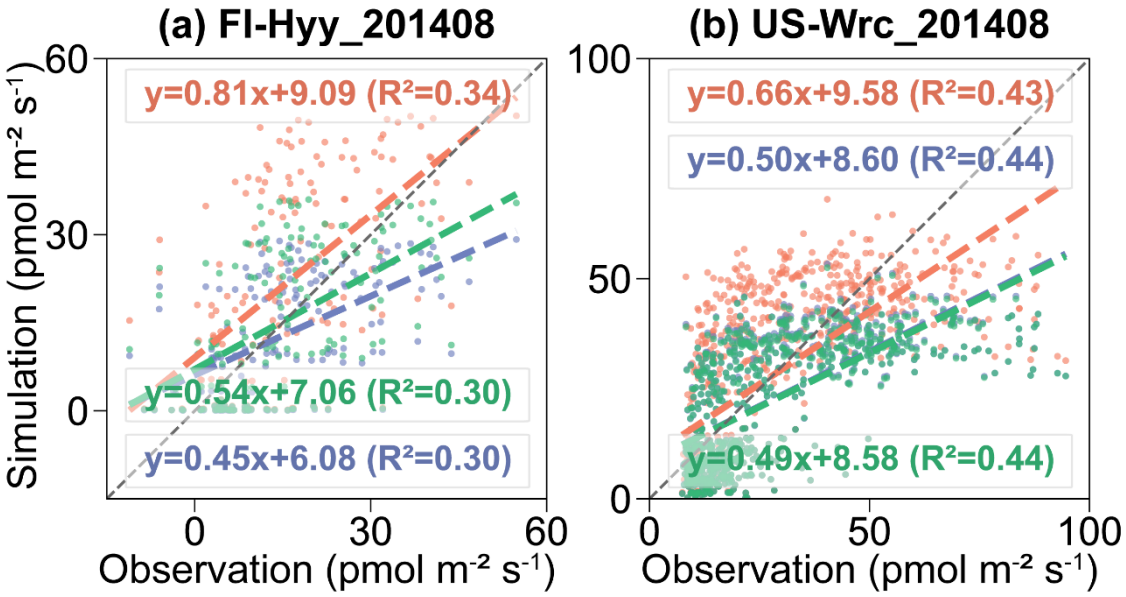

25 **Figure S2.** Hourly scatterplots of observed versus simulated hourly COS flux using prior (red), single-site (blue) and two-site (green) posterior parameters.

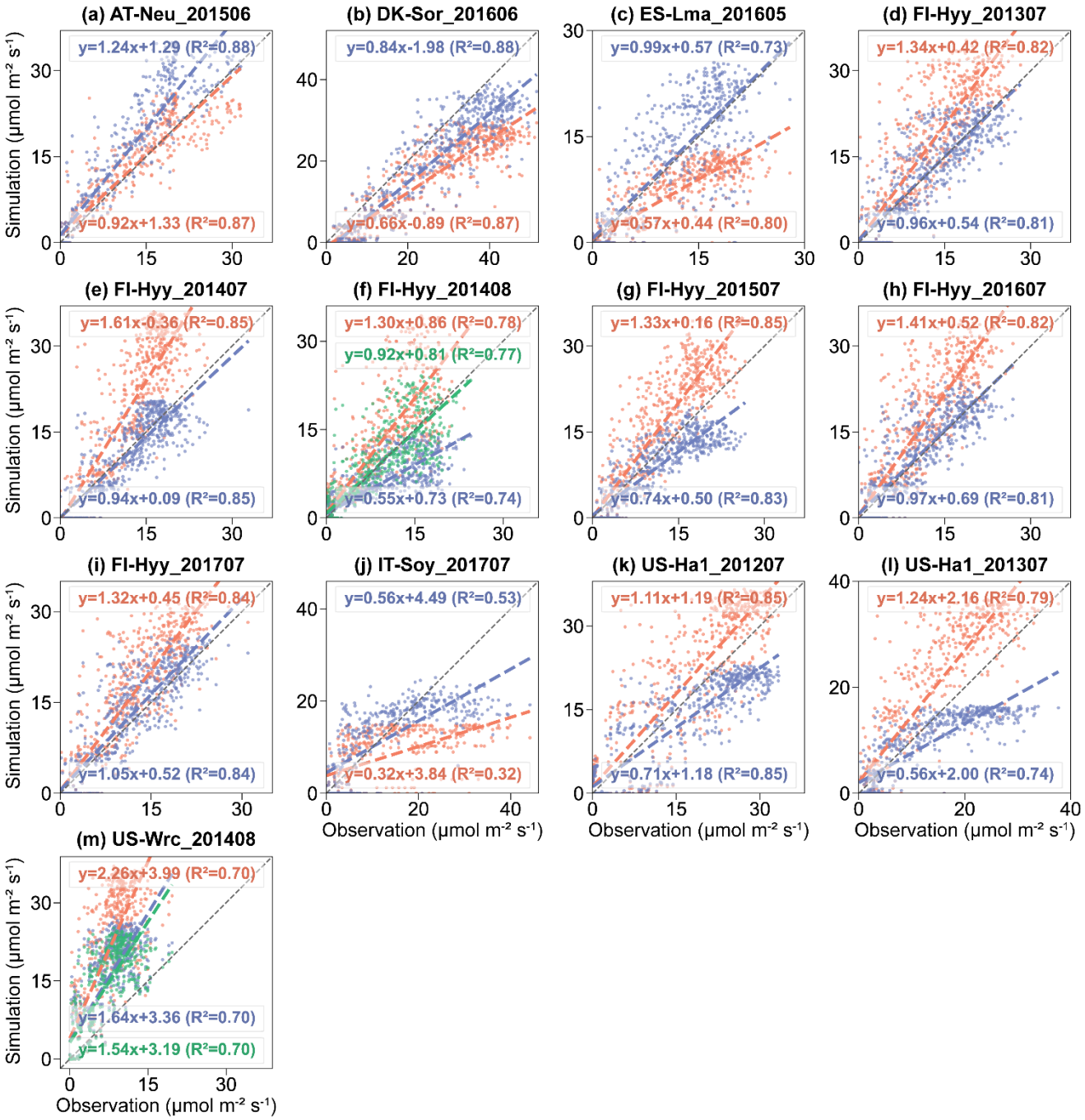

Figure S3. Scatterplots of observed versus simulated hourly GPP using prior (red), single-site (blue) and two-site (green) posterior parameters.

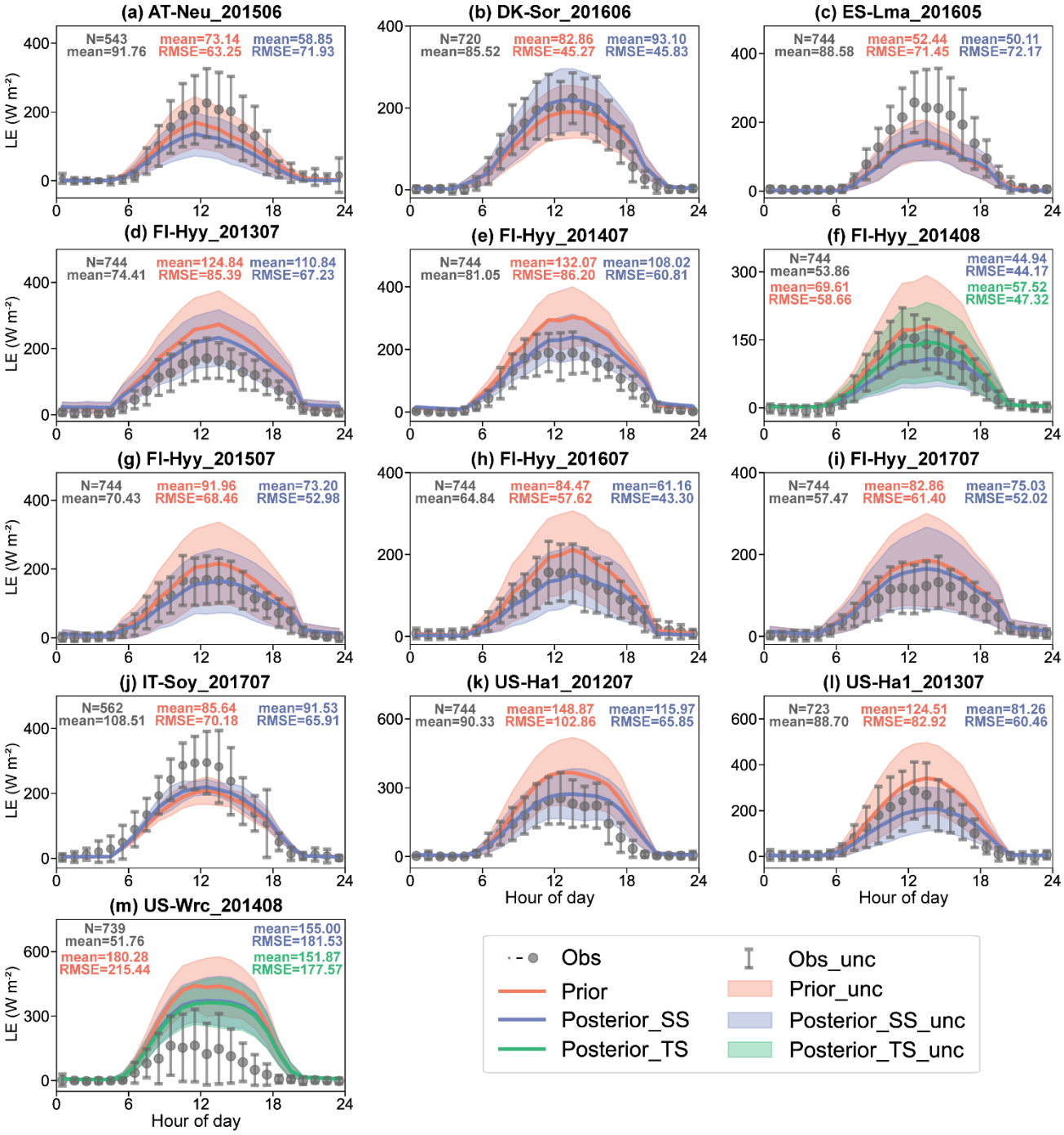

Figure S4. The diurnal cycle of observed (black) and simulated LE using prior parameters (red), single-site (blue) and two-site (green) posterior parameters. The size of the circle indicates the number of observations within each circle (ranging from 1 to 31), and the error bars depict the standard deviations in the mean of observations from the variability within each circle. Lines connect the mean values of simulations and pale bands depict the standard deviation in the mean of simulations from the variability within each bin.

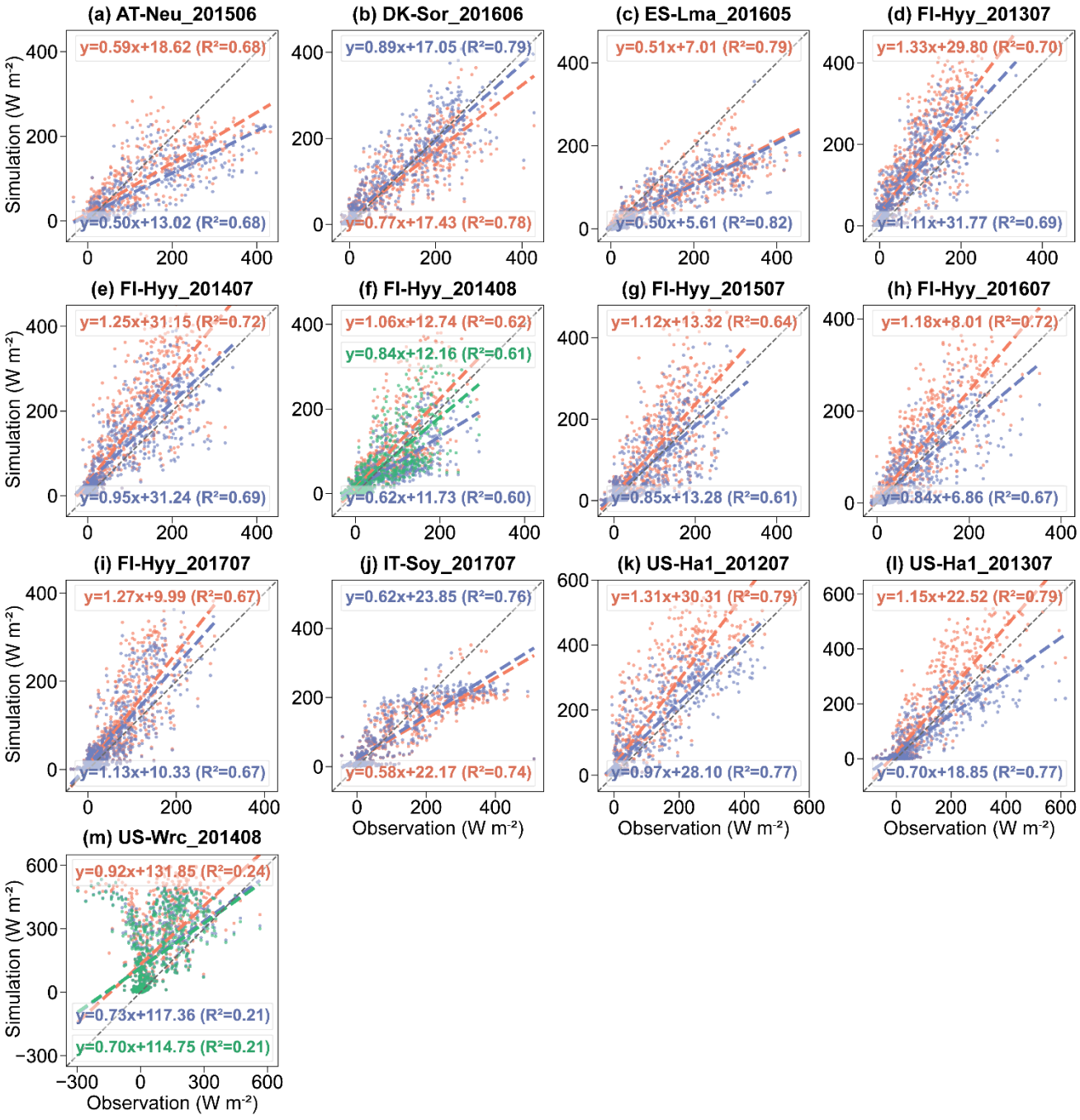

Figure S5. Scatterplots of observed versus simulated hourly LE using prior (red), single-site (blue) and two-site (green) posterior parameters.

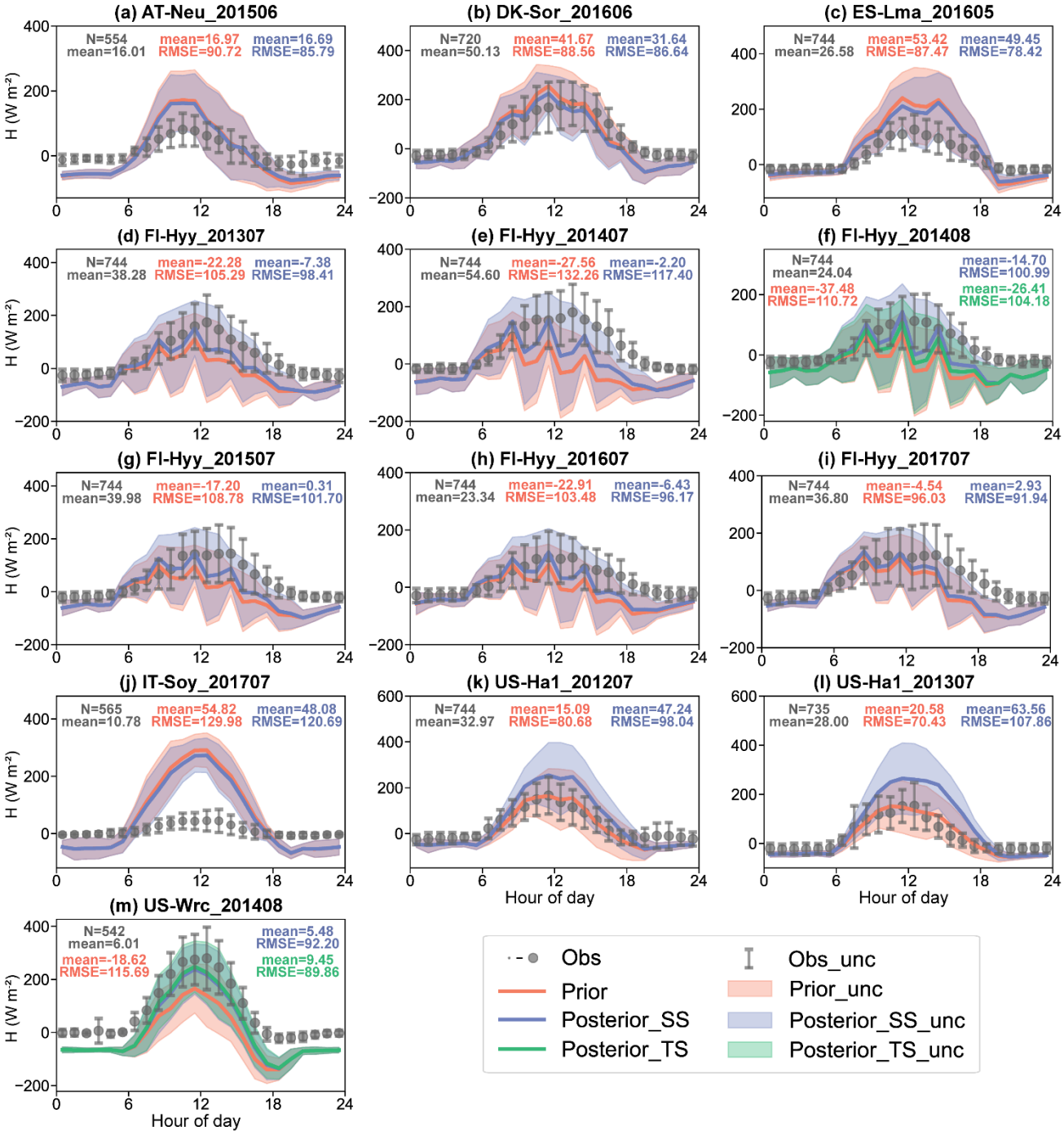

Figure S6. The diurnal cycle of observed (black) and simulated H using prior parameters (red), single-site (blue) and two-site (green) posterior parameters. The size of the circle indicates the number of observations within each circle (ranging from 1 to 31), and the error bars depict the standard deviations in the mean of observations from the variability within each circle. Lines connect the mean values of simulations and pale bands depict the standard deviation in the mean of simulations from the variability within each bin.

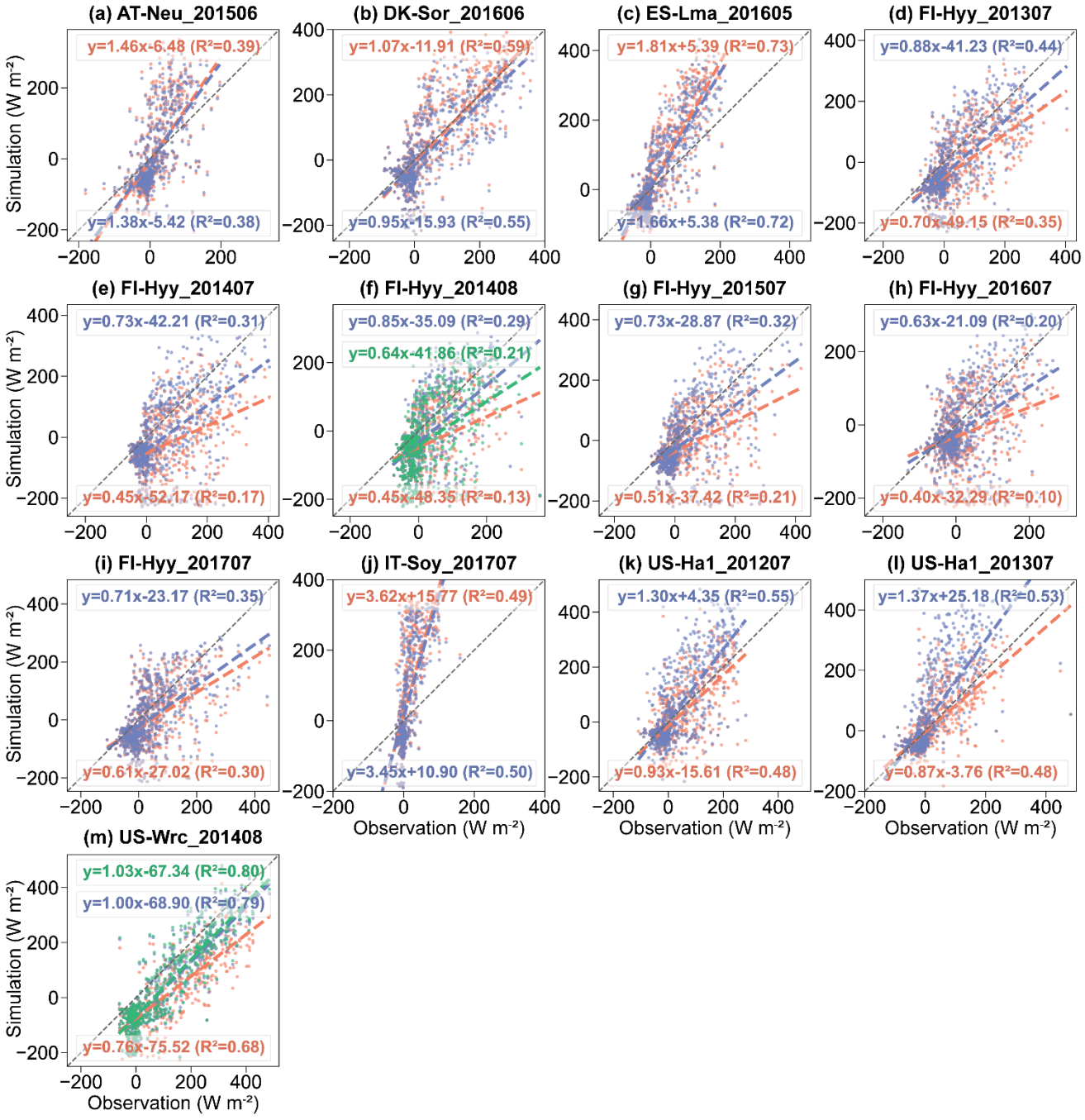

Figure S7. Scatterplots of observed versus simulated hourly H using prior (red), single-site (blue) and two-site (green) posterior parameters.

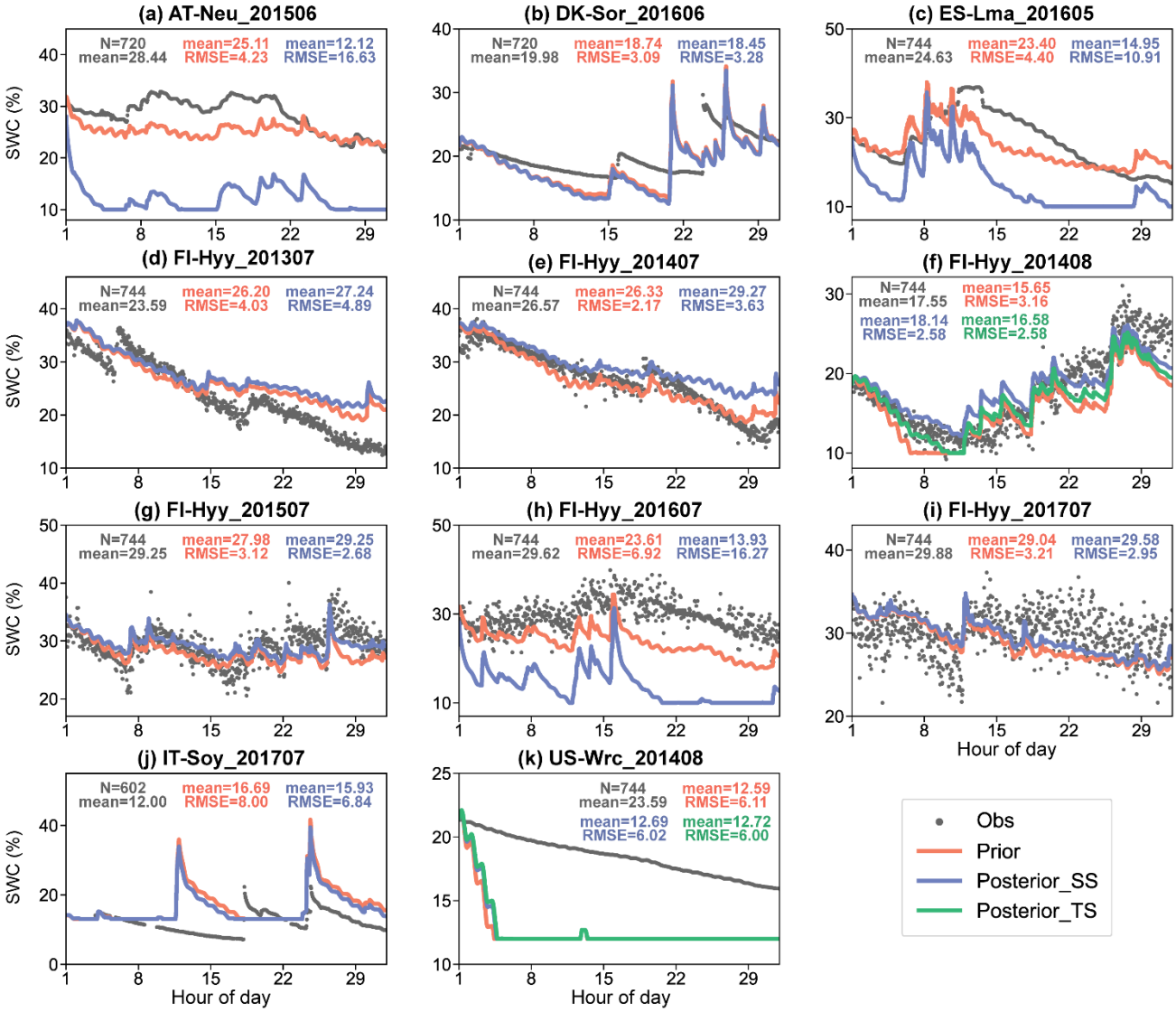

Figure S8. Observed (black point) and simulated SWC (%). Results show SWC simulated using prior parameters (red line), single-site (blue line) and two-site (green line) posterior parameters.

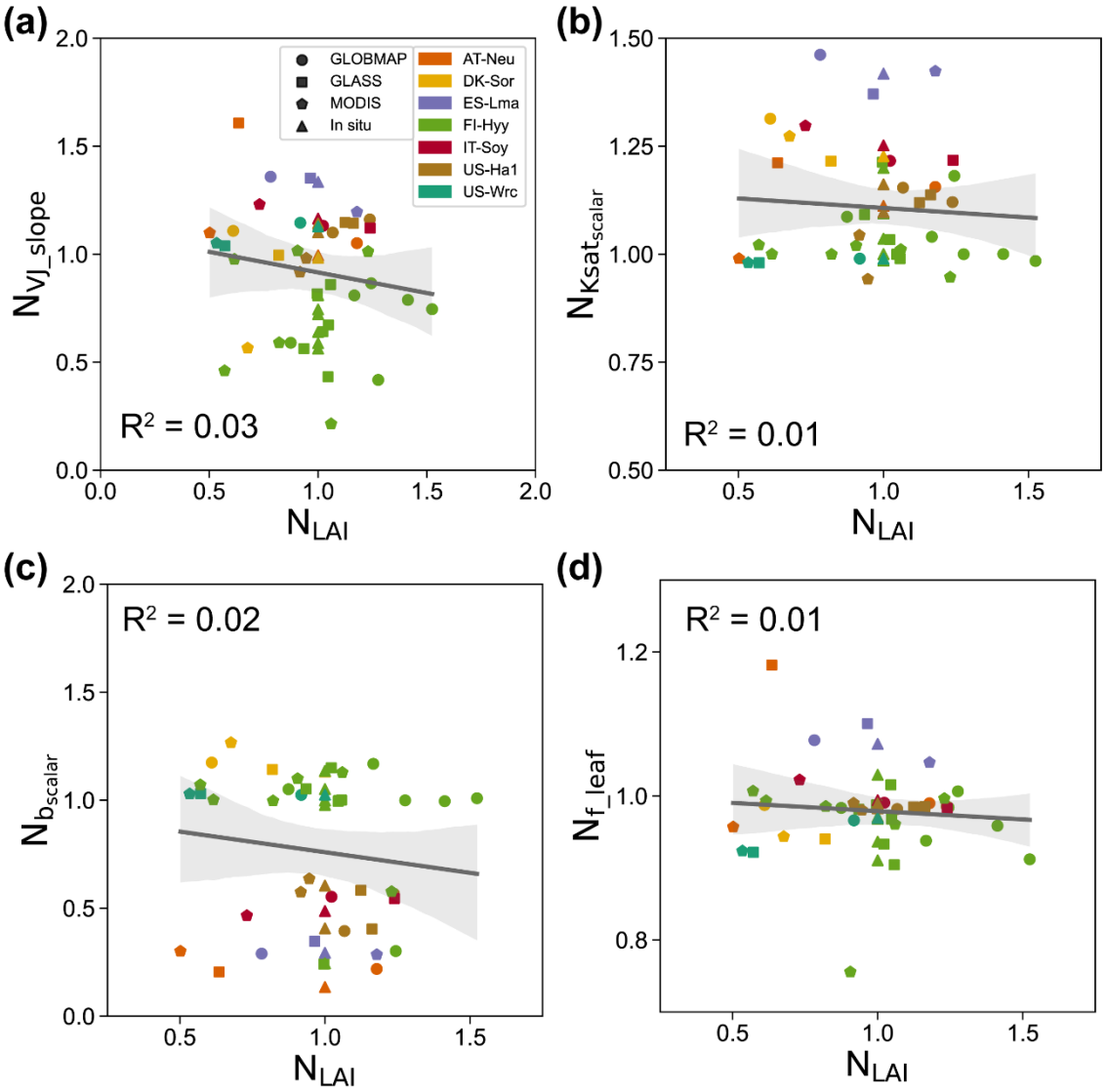

Figure S9. Influence of LAI on the posterior VJ_slope, $Ksat_{scalar}$, b_{scalar} and f_leaf obtained by the single-site experiments conducted at seven sites and driven by four LAI data (GLOBMAP, GLASS, MODIS and *in situ*). The posterior VJ_slope, $Ksat_{scalar}$, b_{scalar}, f_leaf and the LAI were represented by their normalized values N_{VJ_slope}, $N_{Ksat_{scalar}}$, $N_{b_{scalar}}$, N_{f_leaf} and N_{LAI}, respectively. The posterior parameters were normalized by their prior values and the LAI were normalized by the *in situ* values. The linear regression fit line of the posterior parameters obtained based on the satellite-derived LAI (GLOBMAP, GLASS and MODIS) with the corresponding LAI data is shown, with 95% confidence interval spread around the line.

Table S1. PFT and Soil Texture descriptions in BEPS model.

PFT No.	Descriptions
1	Evergreen needleleaf forest
2	Deciduous needleleaf forest

3	Deciduous broadleaf forest
4	Evergreen broadleaf forest
5	Mixed forest
6	Shrub
7	C3 grass
8	C3 crop
9	C4 grass
10	C4 crop

Soil texture No.	Description
1	Sand
2	Loamy sand
3	Sandy loam
4	Loam
5	Silt loam
6	Sandy clay loam
7	Clay loam
8	Silty clay loam
9	Sandy clay
10	Silty clay
11	Clay

Table S2. $alpha$ and $beta$ parameters for COS abiotic flux term.

Site name	PFT in BEPS	PFT in Whelan et al. (2016)	$alpha$ (unitless)	$beta$ (℃$^{-1}$)
AT-Neu	C3 grass	Savanna	-9.54	0.108
ES-Lma	C3 grass	Savanna	-9.54	0.108
DK-Sor	Deciduous broadleaf forest	Temperate forest	-7.77	0.119
US-Ha1	Deciduous broadleaf forest	Temperate forest	-7.77	0.119
FI-Hyy	Evergreen needleleaf forest	Temperate forest	-7.77	0.119
US-Wrc	Evergreen needleleaf forest	Temperate forest	-7.77	0.119
IT-Soy	C3 crop	Soy field	-6.12	0.096

Table S3. Parameters for COS biotic flux term.

PFT in BEPS	PFT in (Whelan et al., 2022)	SWC_{opt} (%)	F_{opt} (pmol m^{-2} s^{-1}) with temperature (℃) at SWC_{opt}	SWC_g (%)	F_{opt} (pmol m^{-2} s^{-1}) with temperature (℃) at SWC_g
C3 grass	Grassland	12.5	F_{opt}: -4.5 F_{T_g}: -1.5 T_{opt}: -10.9	26.9	F_{opt}: -2.3 F_{T_g}: -1.3 T_{opt}: -14.8

			T_g: -25		T_g: -25
Deciduous broadleaf forest	Forest - Temperate or broadleaf	24.6	12.6	51	-0.18T+0.48
Evergreen needleleaf forest	Forest – Boreal or needleleaf	12.5	F_{opt}: -18 F_{T_g}: -12 T_{opt}: 28 T_g: 35	19.3	F_{opt}: -5.9 F_{T_g}: -3.8 T_{opt}: 28 T_g: 35
C3 crop	Agricultural	17.7	-9.7	22	-5.36

Table S4. Description of parameters used for optimizations within the Nanjing University Carbon Assimilation System (NUCAS). Parameters are either specified per PFT, per soil texture, or globally, i.e., all PFTs and textures share one value, as indicated in column 3.

No.	Parameter	Dependent	Unit	Description	Prior Value	Prior Uncertainty
1	V_{cmax25}	PFT	μmol m^{-2} s^{-1}	Maximum carboxylation rate of Rubisco at 25℃	62.5	15.625
2					39.1	9.775
3					57.7	14.425
4					29	7.25
5					66	16.5
6					57.85	14.4625
7					48	12
8					84.5	21.125
9					30	7.5
10					30	7.5
11	VJ_slope	PFT	unitless	Slope of the V_{cmax} and J_{max} (maximum electron transport rate) relationship	2.39	0.5975
12					2.39	0.5975
13					2.39	0.5975
14					2.39	0.5975
15					2.39	0.5975
16					2.39	0.5975
17					2.39	0.5975
18					2.39	0.5975
19					2.39	0.5975
20					2.39	0.5975
21	Q10	PFT	unitless	Soil respiration temperature factor	0.046	0.0115
22					0.046	0.0115
23					0.046	0.0115
24					0.046	0.0115
25					0.046	0.0115
26					0.046	0.0115
27					0.046	0.0115

28					0.046	0.0115
29					0.046	0.0115
30					0.046	0.0115
31	SIF_alpha	PFT	W m^{-2}	Quadratic term coefficient for the relationship between additional heat dissipation under light adapted conditions and relative reduction of photochemical yield	6.2473	1.561825
32					6.2473	1.561825
33					6.2473	1.561825
34					6.2473	1.561825
35					6.2473	1.561825
36					6.2473	1.561825
37					6.2473	1.561825
38					6.2473	1.561825
39					6.2473	1.561825
40					6.2473	1.561825
41	SIF_beta	PFT	W m^{-2}	Primary term coefficient for the relationship between additional heat dissipation under light adapted conditions and relative reduction of photochemical yield	0.5994	0.14985
42					0.5994	0.14985
43					0.5994	0.14985
44					0.5994	0.14985
45					0.5994	0.14985
46					0.5994	0.14985
47					0.5994	0.14985
48					0.5994	0.14985
49					0.5994	0.14985
50					0.5994	0.14985
51	$Ksat_{scalar}$	texture	unitless	Scaling factor of saturated hydraulic conductivity (Ksat)	1	0.25
52					1	0.25
53					1	0.25
54					1	0.25
55					1	0.25
56					1	0.25
57					1	0.25
58					1	0.25
59					1	0.25
60					1	0.25
61					1	0.25
62	b_{scalar}	texture	unitless	Scaling factor of Campbell parameter b (the exponential parameter of Campbell's soil moisture retention model)	1	0.25
63					1	0.25
64					1	0.25
65					1	0.25
66					1	0.25
67					1	0.25
68					1	0.25

69					1	0.25
70					1	0.25
71					1	0.25
72					1	0.25
73	f_leaf	global	unitless	The ratio of photosynthetically active radiation to shortwave radiation	0.466	0.033
74	kc25	global	μbar	Michaelis–Menten constants for CO_2 in 25 ℃	274.6	68.65
75	ko25	global	mbar	Michaelis–Menten constants for O_2 in 25 ℃	419.8	104.95
76	tau25	global	unitless	The CO_2/O2 specificity factor, which reflects the carbon assimilation efficiency of Rubisco	2904.12	726.03

Table S5. Summary of configurations of twin experiments. $J_{initial}$ and J_{final} denote the initial value and the final value of the cost function $J(x)$ respectively; $G_{initial}$ and G_{final} denote the initial value and the final value of the gradient respectively; $D_{initial}$ and D_{final} denote the initial value and the final value of the respectively. D_{final} denote the final value of the distance (D_x) between the parameter vector and the prior parameter vector. The initial value ($D_{initial}$) of D_x for all twin experiments is 7.48, due to an identical perturbation size (0.2) being applied. The suffix "*" indicates the two-site experiment.

Site name	Data duration	$J_{initial}$	J_{final}	$G_{initial}$	G_{final}	D_{final}	Relative changes of parameters (%)				
							V_{cmax25}	VJ_slope	$Ksat_{scalar}$	b_{scalar}	f_leaf
AT-Neu	June 2015	55.08	6.52E-16	48.09	6.65E-07	1.48E-07	-8.13E-10	-3.16E-09	-6.88E-10	-1.68E-09	1.24E-09
DK-Sor	June 2016	77.13	7.45E-16	77.01	1.30E-06	1.70E-08	1.55E-09	-8.85E-10	-2.82E-09	-1.08E-09	-1.80E-09
ES-Lma	May 2016	53.01	3.34E-15	51.59	1.55E-06	8.80E-10	-1.06E-09	1.88E-09	8.54E-09	7.58E-09	4.26E-11
FI-Hyy	July 2013	73.44	2.02E-17	70.43	1.10E-06	2.57E-08	1.29E-10	3.66E-10	-9.30E-11	4.46E-10	-2.01E-10
	July 2014	77.59	1.06E-17	76.83	2.97E-07	4.74E-09	3.18E-10	-6.80E-10	-2.08E-11	-1.96E-10	-1.56E-10
	August 2014	74.09	9.27E-18	70.00	4.63E-07	1.02E-09	-7.33E-11	1.22E-10	5.99E-10	4.59E-10	2.20E-10
	July 2015	72.76	1.19E-16	70.07	7.93E-07	7.58E-10	-1.16E-10	-4.87E-10	1.14E-11	7.20E-10	1.07E-09
	July 2016	75.89	1.13E-18	73.35	2.12E-07	4.53E-08	-9.64E-11	1.08E-10	3.16E-11	3.95E-11	-5.55E-12
	July 2017	73.94	8.47E-17	73.64	7.18E-07	2.45E-08	8.68E-11	7.31E-10	3.69E-12	2.01E-10	8.47E-10
IT-Soy	July 2017	50.75	5.09E-13	38.82	4.94E-07	6.98E-08	2.86E-09	-7.41E-09	2.74E-09	-5.89E-09	-5.70E-10
US-Ha1	July 2012	66.15	1.93E-19	59.66	2.05E-07	1.63E-07	-6.01E-12	7.29E-11	1.35E-11	7.87E-11	-5.81E-12
	July 2013	66.50	1.61E-17	60.25	9.99E-07	2.36E-08	4.42E-09	7.44E-10	-9.77E-11	4.07E-10	-3.52E-11
US-Wrc	August 2014	58.97	3.28E-18	46.87	1.45E-07	2.84E-08	-1.16E-10	4.40E-10	1.22E-10	-7.50E-11	6.04E-11
FI-Hyy*	August 2014	108.04	3.95E-15	119.27	1.28E-06	2.01E-08	-1.16E-10	4.40E-10	1.22E-10	-7.50E-11	6.04E-11
US-Wrc*									-3.41E-10	4.63E-10	

References

Whelan, M. E., Hilton, T. W., Berry, J. A., Berkelhammer, M., Desai, A. R., and Campbell, J. E.: Carbonyl sulfide exchange in soils for better estimates of ecosystem carbon uptake, Atmospheric Chemistry and Physics, 16, 3711-3726, 2016.

Whelan, M. E., Shi, M., Sun, W., Vries, L. K. d., Seibt, U., and Maseyk, K.: Soil carbonyl sulfide (OCS) fluxes in terrestrial ecosystems: an empirical model, Journal of Geophysical Research: Biogeosciences, 127, e2022JG006858, 2022.